



# Effects of terpenes on fluidity and lipid extraction in phospholipid membranes



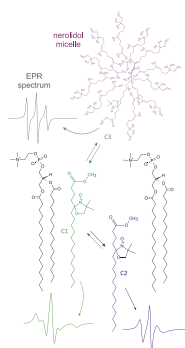
Sebastião Antonio Mendanha, Antonio Alonso\*

Instituto de Física, Universidade Federal de Goiás, Goiânia, GO, Brazil

## HIGHLIGHTS

- Terpenes increase the overall lipid dynamics in phospholipid membranes.
- Lipid extraction from a model membrane by terpenes is characterized.
- The thermodynamic profile associated with the terpene-membrane interactions is presented.

## GRAPHICAL ABSTRACT



## ARTICLE INFO

### Article history:

Received 16 November 2014  
Received in revised form 29 January 2015  
Accepted 1 February 2015  
Available online 7 February 2015

### Keywords:

Electron paramagnetic resonance  
Terpenes  
Membrane fluidity  
Lipid extraction

## ABSTRACT

Electron paramagnetic resonance (EPR) spectroscopy was used in a detailed study of the interactions of several terpenes with DPPC membranes. EPR spectra of a spin-label lipid allowed the identification of two well-resolved spectral components at temperatures below and above the main phase transition of the lipid bilayer. Terpenes caused only slight mobility increases in each of these spectral components; however, they substantially increased the population of the more mobile component. In addition, the terpenes reduced the temperature of the main phase transition by more than 8 °C and caused the extraction of the spin-labeled lipid. Nerolidol, which had the highest octanol–water partition coefficient, generated the highest amount of spin label extraction. Acting as spacers, terpenes should cause major reorganization in cell membranes, leading to an increase in the overall molecular dynamics of the membrane. At higher concentrations, terpenes may cause lipid extraction and thus leakage of the cytoplasmic content.

© 2015 Elsevier B.V. All rights reserved.

## 1. Introduction

Terpenes are volatile substances that are primarily extracted from vegetable oils, and their molecular components include only carbon, hydrogen and oxygen atoms. Terpenes are composed of isoprene units arranged in either linear chains or rings, and they function mainly as chemoattractants or chemorepellents [1,2]. Many dietary terpenes

have shown antitumor activity and are effective in the prevention and chemotherapy of cancer [2–8]. Furthermore, essential oils, or the terpenes contained therein, have shown activity against bacteria, fungi, parasites and viruses [7,8], including the antifungal activity of the monoterpene terpinen-4-ol [9] and the antileishmanial activity of limonene [10] and nerolidol [11].

The electron paramagnetic resonance (EPR) spectroscopy of spin labels has been employed to investigate the mechanisms by which monoterpenes act as enhancers of skin permeation [12–15]. The intercellular lipid matrix of the outermost skin layer, the stratum corneum,

\* Corresponding author. Fax: +55 62 3521 1014.  
E-mail address: [alonso@ufg.br](mailto:alonso@ufg.br) (A. Alonso).

which is the major permeability barrier of the skin, becomes more fluid in the presence of the monoterpenes L-menthol and 1,8-cineole [12,13], and several monoterpenes increase the membrane partition coefficients of the small water-soluble spin labels TEMPO and DTBN in stratum corneum membranes [14,15]. Recently, EPR spectroscopy has been used to show that terpenes can cause pronounced increases in the plasma membrane fluidity of *Leishmania amazonensis* promastigotes at terpene concentrations similar to those that inhibit the growth of the parasite [16]. In addition, the terpenes nerolidol, (+)-limonene,  $\alpha$ -terpineol and 1,8-cineole at concentrations that inhibited the growth of *Leishmania* parasites by 50% caused cell lysis of 4 to 9%, and this percentage rose to approximately 50% for concentrations that were double or triple the  $IC_{50}$  values [16]. The cytotoxicity of seven monoterpenes and the sesqui-terpene nerolidol in cultured fibroblast cells also correlates with the hemolytic potential of these terpenes [17].

With the main objective of understanding the interactions of terpenes with the lipid component of cell membranes, we measured the EPR spectra of spin labels in pure DPPC model membranes to study the effects of a sesquiterpene and three monoterpenes on lipid bilayers, and we primarily focused on the temperature dependence of the molecular dynamics and lipid extraction at three terpene concentrations.

## 2. Materials and methods

### 2.1. Chemicals

The terpenes 1,8-cineole,  $\alpha$ -terpineol, (+)-limonene and nerolidol were purchased from Acros Organics (Geel, Belgium). The spin labels 5-doxyl-stearic acid methyl ester (5-DMS), 16-doxyl-stearic acid methyl ester (16-DMS), 5-doxyl-stearic acid (5-DSA) and 12-doxyl-stearic acid (12-DSA) were purchased from Sigma-Aldrich (St. Louis, USA), and the phospholipid 1,2-dipalmitoyl-sn-glycero-3-phosphocholine (DPPC) was purchased from Avanti Polar Lipids Inc. (Alabaster, USA) (Fig. 1). The other reagents were purchased from Sigma-Aldrich or Merck SA (Rio de Janeiro, Brazil) at the highest available purity.

### 2.2. Preparation and spin labeling of DPPC membranes

DPPC and the spin label were dissolved in chloroform at 1 mg/mL and 5  $\mu$ g/mL (DPPC:spin label molar ratio of  $\sim$ 100:1), respectively, to prepare a film composed of these lipids in the bottom of a glass tube. After an aliquot (50  $\mu$ L) of the organic solvent was applied to the glass tube, the solvent was evaporated using a stream of gaseous nitrogen.

The films were stored under vacuum for 12 h and subsequently hydrated at 55 °C with 200  $\mu$ L of phosphate buffered saline (5 mM phosphate, 150 mM NaCl, pH 7.4) to form a multilamellar suspension of DPPC. Unilamellar vesicles were prepared using a mini-extruder purchased from Avanti Polar Lipids Inc. (Alabaster, USA) and polycarbonate filters with 0.1  $\mu$ m diameter pores. Subsequently, the vesicle suspension was centrifuged (1000  $\times$ g for 10 min) to increase the concentration to approximately 50 mM DPPC, and the final volume decreased to  $\sim$ 50  $\mu$ L.

The terpenes were diluted in ethanol to a terpene:ethanol ratio of 1:2 (v/v), and aliquots of this solution were added to unilamellar vesicles of DPPC. The ethanol concentration necessary to deliver the highest terpene concentration used in the sample was 3% (v/v); this ethanol concentration does not affect DPPC membrane fluidity.

After homogenization, the membranes were introduced in capillary tubes with an internal diameter of 1 mm, which were sealed using a flame. Finally, the samples were preheated to 45 °C for 30 min before the EPR experiments.

### 2.3. EPR spectroscopy

EPR measurements were conducted using a Bruker ESP300 spectrometer (Rheinstetten, Germany), operating in the X-band (approximately 9.4 GHz) with an ER4102 ST resonant cavity and a Bruker system for temperature control. To improve the thermal stability of the samples, the capillaries containing DPPC vesicles were dipped in mineral oil inside the quartz tube used to position the sample within the resonant cavity. A thermocouple was inserted into the quartz tube and was in contact with the oil at a position slightly above the center of the cavity to increase the precision when measuring the temperature of the sample. The EPR measurements were performed using the following instrumental parameters: microwave power, 2 mW; modulation frequency, 100 kHz; amplitude of modulation, 1 G; magnetic field scan, 100 G; scan time, 168 s and detection time constant, 41 ms.

### 2.4. Spectral simulation

The simulation of the EPR spectra was performed using the nonlinear least-squares (NLS) software developed by Freed JH et al. [18,19]. In this work, it was assumed that the rotational diffusion tensor  $R$  of the labeled molecule has axial symmetry with its principal molecular axis ( $z$  axis of the nitroxide radical) in the direction perpendicular to the plane of the lipid bilayer, and the axial rotational anisotropy was defined by the relationship  $N = \log(R_{\parallel}/R_{\perp}) = 1$ . The rate of rotational Brownian diffusion,

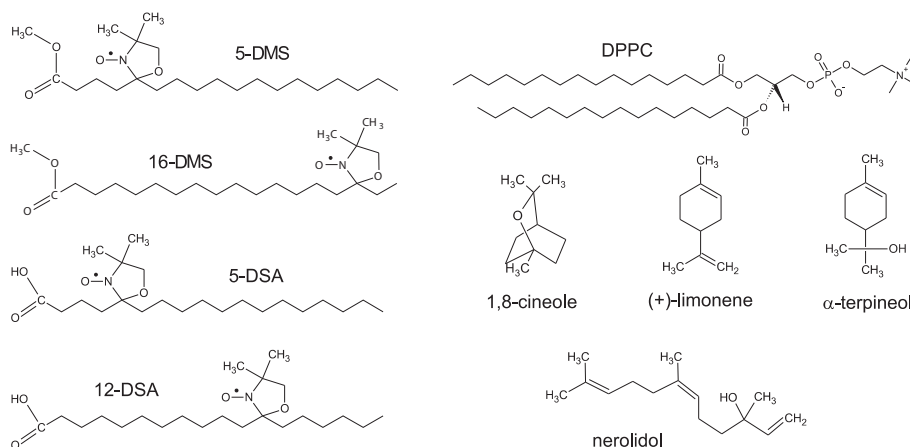


Fig. 1. Chemical structures of the lipid, spin labels and terpenes used in this work.

$R_{bar}$ , obtained from the NLLS program was converted to the rotational correlation time,  $\tau_c$ , through the following relationship [18]:

$$\tau_c = \frac{1}{6R_{bar}} \quad (1)$$

The theoretical spectra were fitted to the experimental spectra using models containing one or two spectral components. As in other studies [20,21], the magnetic parameters were determined based on a global analysis of all the spectra obtained in this work. Once the parameters were determined, all of the spectra were simulated using the same input parameters for the magnetic tensors  $g$  and  $A$ :  $g_{xx}(1) = 2.0080$ ;  $g_{yy}(1) = 2.0060$ ;  $g_{zz}(1) = 2.0017$ ;  $A_{xx}(1) = 6.9$ ;  $A_{yy}(1) = 6.0$ ;  $A_{zz}(1) = 32.0$ ;  $g_{xx}(2) = 2.0082$ ;  $g_{yy}(2) = 2.0062$ ;  $g_{zz}(2) = 2.0027$ ;  $A_{xx}(2) = 5.7$ ;  $A_{yy}(2) = 5.6$ ; and  $A_{zz}(2) = 31.2$ , in which the numbers (1) and (2) indicate the first and second spectral component, respectively.

### 3. Results

#### 3.1. Analysis of the spectral components

As demonstrated in the work by Camargos and Alonso [22], the spectra of spin labels, such as 5-DMS in DPPC membranes, can be fitted as the superposition of two spectral components with characteristic line shapes, motion parameters and polarities. In this study, we used the approach of Camargos and Alonso [22]. It has been demonstrated that when the cholesterol hydroxyl group is replaced with a ketone group, the interaction of the new molecule with the polar groups of the DPPC bilayer is reduced, leading to unstable positioning of the molecule in the membrane [23]. In this approach, the spin label can be in one of two major positions when incorporated into lipid bilayers; moreover, a third position associated with the spin label outside of the membrane was added (Fig. 2). We use the term spectral component 1 (C1) for the fraction of the spin label in DPPC membranes that strongly interacts with the polar groups of the bilayer and the term spectral component 2 (C2) for the fraction of the spin labels that are located more deeply in the membrane and therefore interact weakly with the polar interface. Finally, we use the term spectral component 3 (C3) for the fraction of spin label outside of the DPPC bilayers and incorporated into the micelles formed by the terpene molecules. Given the technical difficulty in simulating EPR spectra using three components, we performed simulations using a model of at most two spectral components; this model only accounted for the two main components of the spectra, and the contribution of the third component, with a smaller population, was considered negligible. Thus, the simulations were performed using two combinations of components: C1 and C2 or C1 and C3. The spin labels of C1 (strong interaction with the membrane polar groups) show a broad line profile, indicating slower and anisotropic motion, and the probes of C2 (weak interaction with the membrane polar interface) have narrower and less anisotropic lines that result from a higher degree of movement. The probes of C3 show faster molecular motion and resonance lines that are even narrower than those of C2 (Fig. 2).

Fig. 3 shows the most representative experimental spectra, their best fits and the respective spectral components of 5-DMS in pure DPPC membranes (control sample, Fig. 3A) and in membranes treated with terpene (Fig. 3B) at the terpene:lipid molar ratio of 0.8:1 (total molar ratio in the suspension) and the temperature intervals  $\alpha$ ,  $\beta$  and  $\gamma$  ( $\alpha = 0$ – $20^\circ\text{C}$ ,  $\beta = 20$ – $45^\circ\text{C}$ , and  $\gamma = 45$ – $80^\circ\text{C}$ ). Similar figures for other terpene:lipid molar ratios (0.6:1 and 1.2:1) are shown in the supplementary material (Figs. SM1 and SM2). In general, the presence of terpenes facilitates the transfer of the spin label from C1 to C3 in the interval  $\alpha$  and from C1 to C2 in the intervals  $\beta$  and  $\gamma$ . For example, the spectra for the membranes treated with 1,8-cineole, (+)-limonene and nerolidol in the temperature interval  $\alpha$  with a terpene:lipid molar ratio of 0.8:1 can be described as a superposition of C1 and C3. In

contrast, for the control (pure DPPC membrane) and  $\alpha$ -terpineol-treated samples, the experimental spectra are fitted using only C1. For the  $\beta$  and  $\gamma$  temperature ranges, the spectra of pure DPPC membranes and the spectra of all of the terpene-treated membranes can be fitted using a combination of C1 and C2 (Fig. 3B) because the partitioning of terpenes in DPPC membranes should increase with increasing temperature, thereby reducing the formation of micelles, which produce component C3.

To examine whether the ability of terpenes to facilitate the transfer of spin labels from C1 to C3 is also related to the molecular structure of each probe, we recorded EPR spectra at  $10^\circ\text{C}$  for several spin labels that were incorporated into DPPC membranes treated with the monoterpene (+)-limonene (Fig. 4). Note that for the spin labels that have the carbonyl group (5- and 16-DMS), which interact less with the polar groups of the lipid bilayer compared to spin labels that contain a carboxyl group, and are therefore less efficient at forming hydrogen bonds at the polar interface, component 3 is clearly resolved in the EPR spectra for the terpene:lipid total molar ratio of 0.8:1. However, for the spin labels with the carboxyl group (5- and 12-DSA), component 3 is not present in the experimental spectrum. Importantly, increasing the terpene:lipid total molar ratio to 1.2:1 does not alter the 5-DSA spectrum, suggesting that (+)-limonene cannot extract n-DSA-type spin labels from the DPPC bilayer even at the highest terpene concentration used in this work. To further examine the process of lipid extraction by terpenes, we used DPPC as a model biological membrane and the spin label 5-DMS, which can be extracted from DPPC membranes by terpenes. The EPR spectra of both 5-DMS and 5-DSA are very suitable for the analysis of molecular dynamics. However, the weak interaction of 5-DMS with the polar groups of the DPPC bilayer allows it to be displaced to the C2 and C3 components more easily. DPPC is a very well characterized biological membrane model, and the temperature of its main phase transition ( $T_m = 41.4^\circ\text{C}$  [24]) is relatively high, allowing a comprehensive analysis of the effects of terpenes in the gel phase.

#### 3.2. Dynamic and thermodynamic profiles of the spectral components

Fig. 5 shows the EPR spectra of 5-DMS in micelles of the terpenes 1,8-cineole, (+)-limonene,  $\alpha$ -terpineol and nerolidol and the plot of the temperature dependence of the rotational correlation time,  $\tau_c$ . This parameter is obtained from the simulation of the EPR spectra and reflects the motion of the spin labels [13,19,22]. As shown, 5-DMS has its highest and lowest degrees of mobility when inserted in the (+)-limonene and  $\alpha$ -terpineol micelles, respectively. Fig. 6 shows the thermal behavior of the motional EPR parameter for 5-DMS in DPPC vesicles treated with terpenes at a terpene:lipid total molar ratio of 0.8:1 (Fig. SM2 of the supplementary material shows the graphics for the molar ratios 0.6:1 and 1.2:1). At temperatures near  $38^\circ\text{C}$ , the addition of terpenes causes a decrease in the  $\tau_{c1}$  and  $\tau_{c2}$  values relative to those of the control sample for all terpene concentrations. This decrease occurs because terpenes reduce the temperature of the main phase transition of the DPPC membranes. However, for temperatures above the main phase transition, the changes were very small, and for temperatures below  $20^\circ\text{C}$  only 1,8-cineole and (+)-limonene caused slight increases in the mobility of component 1. Table 1 shows the  $\tau_c$  values of 5-DMS for components 1, 2 and 3 and for selected temperatures within the temperature ranges  $\alpha$ ,  $\beta$  and  $\gamma$ . Note that for the terpene:lipid ratio of 0.6:1, only the monoterpenes 1,8-cineole and (+)-limonene are able to extract the spin label from the DPPC membranes (presence of a spin label fraction in component 3). Moreover, for the ratio 1.2:1, the sesquiterpene nerolidol caused total extraction of the spin label throughout the studied temperature range. At  $10^\circ\text{C}$ , only nerolidol did not show a tendency to reduce the  $\tau_c$  values compared to the control sample (Table 1). Nerolidol does not cause spin label extraction at a molar ratio of 0.6:1 (Figs. 8 and SM2), suggesting that the spin label remains in the membrane, thus reducing the  $\tau_c$  value

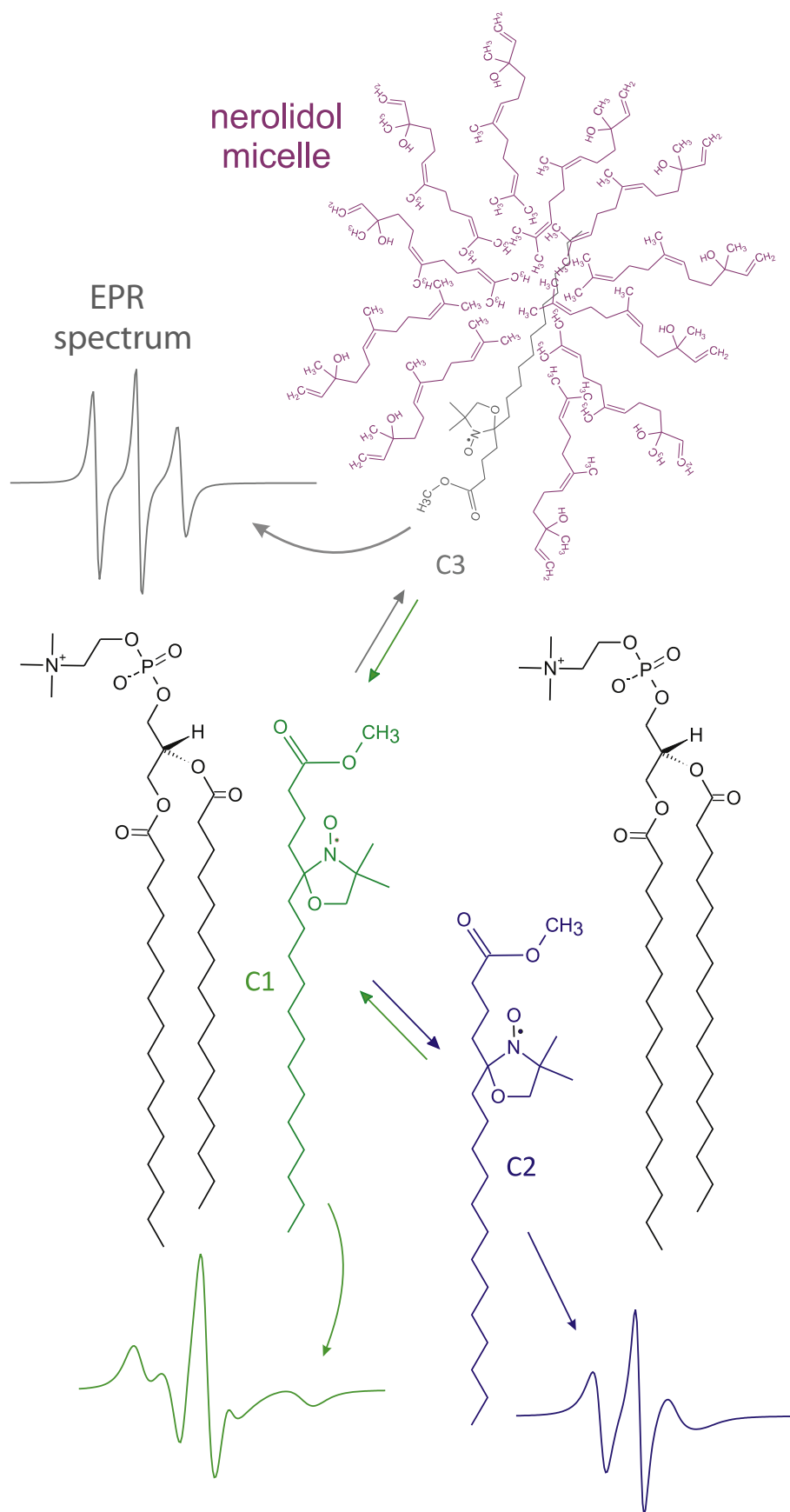


**Fig. 2.** Schematic representation of the proposed positions for the spin label 5-DMS in DPPC membranes treated with terpenes and the corresponding spectral lines. The spin labels from component 1 (green) have their carbonyl group preferentially located in the polar region of the bilayer, whereas the spin labels from component 2 (blue) are inserted more deeply in the membrane and have less restricted motion (weak interaction with the polar interface). The spin labels from component 3 (gray) are not present in the lipid bilayer and are incorporated in aggregates or micelles.

to 7.7 ns. At the higher molar ratio of 0.8:1, nerolidol caused an important extraction, indicating that a greater fraction of spin label molecules are in the formed micelles and, consequently, only a small amount of spin label molecules remain in the membrane; therefore, nerolidol does not increase the fluidity of the membrane at this concentration. It can be noted in Fig. 6 that the  $\tau_c$  values for component C3 are somewhat higher than those observed for terpene micelles, suggesting that the micelles might have some interaction with DPPC vesicles. With increasing temperature, the component C3 progressively turns on component C2. The EPR spectra in Fig. 7 show that the addition of terpenes reduces the temperature of the main phase transition of DPPC membranes ( $\sim 41^\circ\text{C}$ ) to  $26\text{--}34^\circ\text{C}$  (decreases of  $8\text{--}15^\circ\text{C}$ ).

Fig. 8 shows the plots of the thermal dependence of the relative populations of the spectral components of 5-DMS in DPPC membranes treated with the terpenes used in this study. The percentage of component 3 when the spectra were simulated using only components 1 and 3 is plotted for temperatures less than  $20^\circ\text{C}$ ; for temperatures above  $20^\circ\text{C}$ , the fraction of component 1 for spectra simulated with components 1 and 2 is plotted. The gradual increase in temperature generally facilitates the transfer of the spin labels from C1 to C3 or C1 to C2 (depending on the temperature range and the terpene). This finding indicates that component 1 is more stable and that the populations of components 3 and 2 increase through an endothermic process.

Because the relative populations of the spin labels in each spectral component ( $N_1$ ,  $N_2$  and  $N_3$ ) are in thermodynamic equilibrium, the equilibrium constant,  $K_e$ , can be determined for different temperatures when assuming a two-state model. This fact allowed us to calculate the thermodynamic parameters associated with the transfer of the spin label from C1 to C2 or from C1 to C3. The change in the Gibbs free energy of the system,  $\Delta G$ , can be written as follows [25,26]:

$$\Delta G = \Delta G^\circ + RT \ln K_e \quad (2)$$

where  $\Delta G^\circ$  is the change in the standard Gibbs free energy,  $R$  is the universal gas constant, and  $T$  is the absolute temperature. At thermodynamic equilibrium  $\Delta G = 0$ ; therefore, we can derive the following equation:

$$\Delta G^\circ = -RT \ln K_e \quad (3)$$

Using the definition of Gibbs free energy,  $G = H - TS$ , where  $H$  is the enthalpy and  $S$  is the entropy of the system, we can write Eq. (3) as follows:

$$\ln K_e = -\frac{\Delta H^\circ}{RT} + \frac{\Delta S^\circ}{R} \quad (4)$$

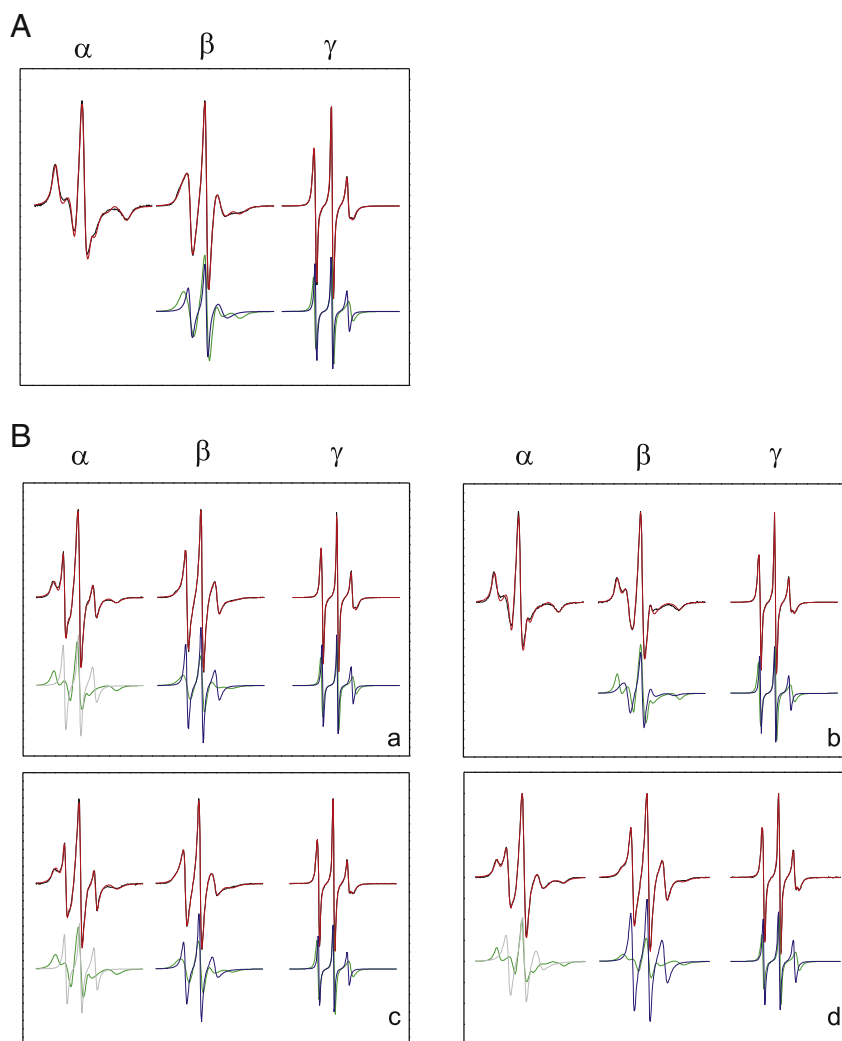


**Fig. 3.** Experimental (black line) and best-fit (red line) EPR spectra of 5-DMS incorporated into pure (panel A) and terpene-treated DPPC vesicles (panel B) for the terpene:lipid total molar ratio of 0.8:1 and temperature ranges of  $\alpha = 0\text{--}20^\circ\text{C}$ ,  $\beta = 20\text{--}45^\circ\text{C}$  and  $\gamma = 45\text{--}80^\circ\text{C}$ . Panels: a, 1,8-cineole; b,  $\alpha$ -terpineol; c, (+)-limonene; d, nerolidol. The green and blue lines represent spectral components 1 and 2, respectively. The gray line represents the signal of the spin labels incorporated into terpene micelles (component 3). The total magnetic field range in each spectrum is 100 G.

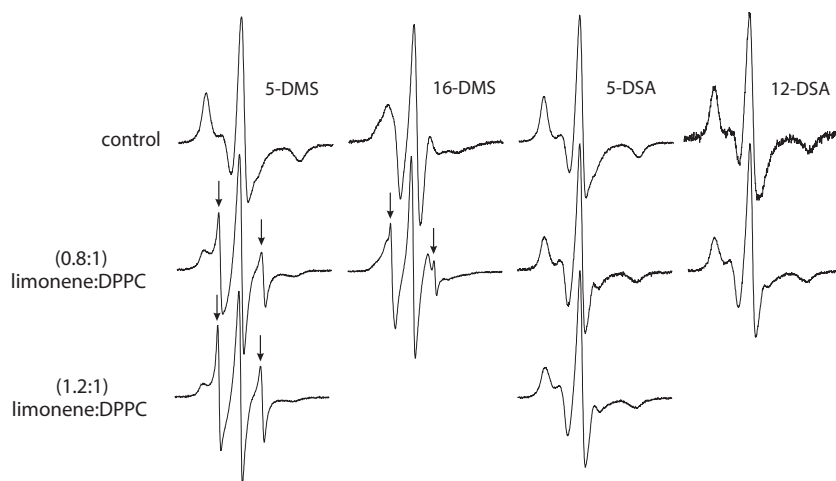


**Fig. 4.** EPR spectra of the spin labels 5-DMS, 16-DMS, 5- and 12-DSA incorporated into DPPC vesicles treated with (+)-limonene at 10 °C. Arrows indicate the magnetic field positions where the resonance lines of component 3 are clearly resolved. The monoterpene can extract the spin labels 5-DMS and 16-DMS but cannot extract 5-DSA or 12-DSA.

with  $\Delta H^\circ$  and  $\Delta S^\circ$  representing the changes in the standard enthalpy and entropy, respectively, associated with the transfer of the spin label from component 1 to 2 or component 1 to 3. Eq. (4), which is known as the van't Hoff equation [26], provides a practical method of determining the thermodynamic parameters of the system by examining  $\ln K_e$  plots as a linear function of  $1/T$  (Fig. 9). In this type of plot, the angular and linear coefficients are equivalent to  $-\frac{\Delta H^\circ}{R}$  and  $\frac{\Delta S^\circ}{R}$ , respectively.

In Fig. 9 for the control sample, there is a clear change in the thermal behavior of the relative populations of C1 and C2 that occurs in the region of  $T_m$ . For temperatures above  $T_m$ , the membranes treated with  $\alpha$ -terpineol or (+)-limonene were essentially equivalent to the control sample, whereas those treated with nerolidol showed a clear increase in C2. Note also that the treatment with 1,8-cineole caused an increase in C2 but only at temperatures just above  $T_m$ . Table 2 shows the values of the thermodynamic parameters associated with the transfer of 5-DMS from C1 to C2 or C1 to C3 in DPPC vesicles treated with the terpenes at terpene:lipid ratios of 0.6:1, 0.8:1 and 1.2:1 only for the temperatures where the components were clearly resolved in the experimental spectrum. The values of  $\Delta G^\circ$  ( $C_1 \rightarrow C_3$ ) for 1,8-cineole and (+)-limonene decrease with increasing concentrations of these monoterpenes, leading to a change in the thermodynamic equilibrium with an increase in population C3 (greater extraction of the spin label). As shown in Fig. 8,  $\alpha$ -terpineol extracted the spin label only at the highest concentration and at temperatures of 14 and 22 °C; in contrast, nerolidol did not induce extraction at the lowest concentration but caused the greatest extraction,  $\Delta G^\circ$  ( $C_1 \rightarrow C_3$ ) = 0.08 kcal/mol, when applied at

the intermediate concentration and caused total extraction at the highest studied concentration. The values of  $\Delta H^\circ$  ( $C_1 \rightarrow C_3$ ) for (+)-limonene are smaller than those for 1,8-cineole, indicating that the transfer of 5-DMS during the extraction process is associated with a lower energy change or a lower reorganization in the membrane-micelle system. In the presence of terpenes, the values of  $\Delta G^\circ$  ( $C_1 \rightarrow C_2$ ) decreased for temperatures below  $T_m$  and above 20 °C, indicating that the addition of the terpene increases the occurrence of component 2 (higher mobility). This change is associated with lower values of  $\Delta H^\circ$  ( $C_1 \rightarrow C_2$ ), indicating an easier transfer of the spin label from C1 to C2 at all studied concentrations. For temperatures above  $T_m$ , the terpenes exhibited smaller effects on the transfer of 5-DMS.

#### 4. Discussion

Two-component EPR spectra are observed for several spin labels in model membranes composed of a single type of phospholipid [21,22]. The behavior of the spin label 5-DMS inserted into phospholipid bilayers with different carbon chain lengths was analyzed, and the results suggested that the spin label can be accommodated in two main energy states in thermodynamic equilibrium, which produce two spectral components [22]. Similar behavior was also observed for lipid spin labels incorporated into stratum corneum membranes [12, 13,21], and the presence of the terpene 1,8-cineole has been shown to favor the formation of the more mobile component in both the stratum corneum and DPPC membranes [13]. Although the lipid matrix of the stratum corneum possesses a complex composition, changes in the

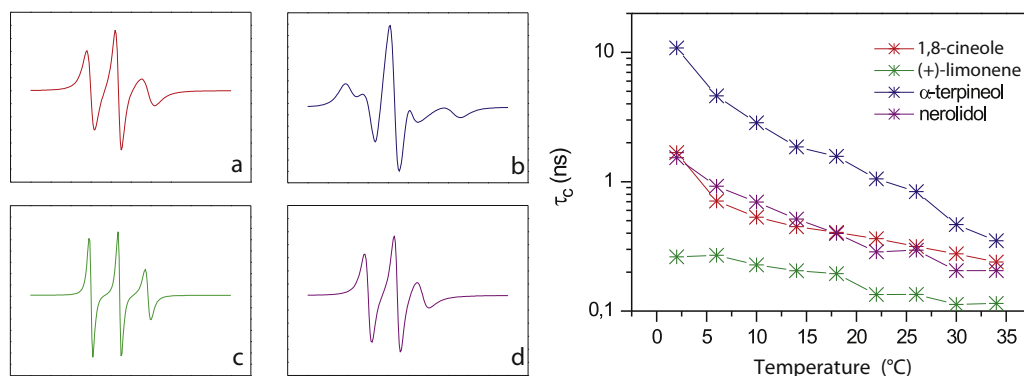


**Fig. 5.** Best-fit EPR spectra of 5-DMS incorporated into terpene micelles (500 mM) at 10 °C (left panel) and the thermal behavior of their rotational correlation times,  $\tau_c$  (right panel). In the left panel: a = 1,8-cineole; b =  $\alpha$ -terpineol; c = (+)-limonene; d = nerolidol.



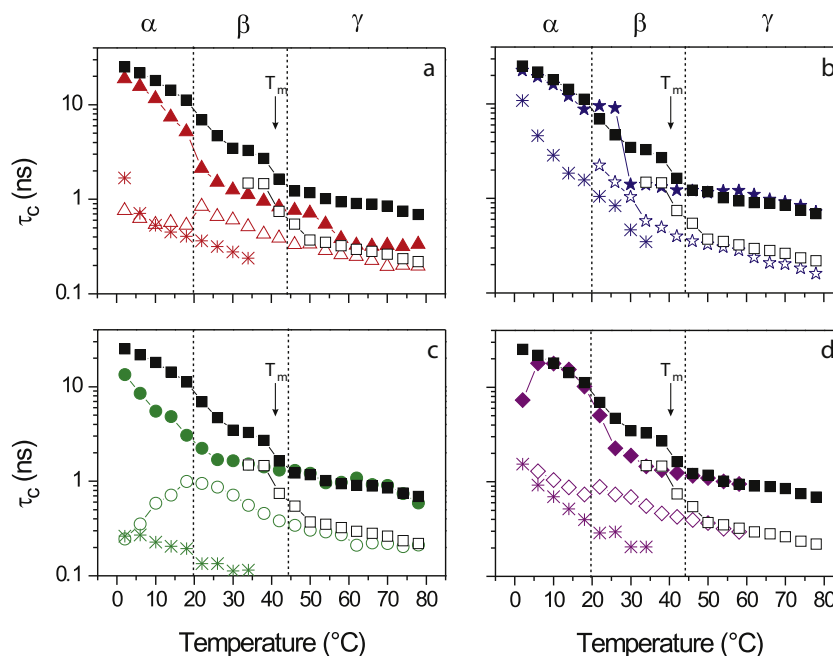


**Fig. 6.** Rotational correlation time,  $\tau_c$ , for 5-DMS embedded in pure and terpene-treated DPPC vesicles at a terpene:lipid total molar ratio of 0.8:1 and temperature ranges  $\alpha = 0$ –20 °C,  $\beta = 20$ –45 °C and  $\gamma = 45$ –80 °C. Panels: a, 1,8-cineole; b,  $\alpha$ -terpineol; c, (+)-limonene; d, nerolidol. Symbols: squares, control sample; triangles, 1,8-cineole; stars,  $\alpha$ -terpineol; circles, (+)-limonene; diamonds, nerolidol. The closed symbols correspond to component 1, and the open symbols correspond to components C2 or C3 (below 20 °C). The asterisks and squares represent the data for 5-DMS in terpene micelles and in pure DPPC (control sample), respectively. The arrows indicate the temperature of the main phase transition ( $T_m = 41.4$  °C) of the control sample.

EPR spectra in the presence of terpenes are consistent with the behavior observed in this work for pure DPPC treated with terpenes. In this work, we observed that terpenes were able to extract the spin label 5-DMS from DPPC bilayers and to accommodate these spin labels in their micelles (component 3). It has been demonstrated that the terpenes carvacrol, linalool and  $\alpha$ -terpineol (5% w/v) in 50% ethanol enhance the permeation of haloperidol through human skin *in vitro* by disrupting the lipid bilayer and extracting the lipids of the stratum corneum [27]. Terpenes in combination with ethanol also increased the permeability of luteinizing hormone releasing hormone through porcine skin by enhancing the extraction of stratum corneum lipids [28]. It has been

shown that the membrane partition coefficients of the small water-soluble spin labels TEMPO and DTBN in the stratum corneum and in DPPC membranes increase with increasing temperature, with the greatest increases for temperatures above the phase transition of the membranes [14,15]. In this work, the EPR signal of 5-DMS in terpene micelles present in the system of DPPC vesicles:terpenes was generally observed for temperatures below 30 °C, suggesting that with increasing temperature more terpenes penetrate in DPPC bilayers, forming a minor amount of micelles.

As demonstrated by Karande et al. [29], the forces responsible for lipid extraction and the potential for skin irritation are proportional to the ability of the molecules to form hydrogen bonds. It has been shown that terpenes, which have –OH or –C=O groups, may weaken the hydrogen bonding network of the stratum corneum membranes, increasing the permeation of imipramine hydrochloride through the skin [30]. Our results indicate that terpenes, which primarily act as spacers, increased the relative population and mobility of the spin-labeled probes in component 2, as shown in Fig. 8 and Table 2 (decreasing values of  $\Delta G^{\circ}_{1 \rightarrow 2}$  and  $\Delta H^{\circ}_{1 \rightarrow 2}$ ); thus, the terpenes were able to decrease the temperature of the main phase transition in DPPC membranes (Fig. 7). This behavior is consistent with the results obtained for the spin labels 5-DMS and 5-DSA in DPPC, DMPC and stratum corneum membranes treated with terpenes [13,22].

The experimental data for the terpenes studied in this work indicate that  $\alpha$ -terpineol caused the smallest extraction of the spin label, and as it has the lowest octanol–water partition coefficient ( $\text{Log}P_{\text{O/W}}$ : (+)-limonene = 3.22; 1,8-cineole = 2.35;  $\alpha$ -terpineol = 2.17 and nerolidol = 4.31) [31], we can deduce that  $\alpha$ -terpineol penetrates less in the membrane and consequently has a smaller capacity to increase the fluidity of DPPC bilayers. Generally,  $\alpha$ -terpineol caused the smallest increases in the membrane dynamics and in the transfer rates of the spin label from component 1 to 2. In addition,  $\alpha$ -terpineol formed micelles that had higher rigidity (Fig. 6), which must have a lower affinity for the spin label; thus,  $\alpha$ -terpineol did not reduce the energy required for transfer of the probe from the lipid bilayers to the micelles. With

**Table 1**

Rotational correlation time,  $\tau_c$ , associated with the components 1, 2 and 3 of 5-DMS incorporated in pure and terpene-treated DPPC membranes at three terpene:lipid total molar ratios (0.6:1, 0.8:1 and 1.2:1). The estimated experimental error of the parameter  $\tau_c$  is 0.2 ns.

Sample		$\tau_c$ (ns)					
		10 (°C)		38 (°C)		50 (°C)	
		C <sub>1</sub>	C <sub>3</sub>	C <sub>1</sub>	C <sub>2</sub>	C <sub>1</sub>	C <sub>2</sub>
1,8-Cineole	0.6:1	17.5	1.1	1.3	0.5	1.0	0.3
	0.8:1	11.6	0.6	1.0	0.4	0.7	0.3
	1.2:1	12.0	0.4	0.7	0.5	0.4	0.3
(+)–Limonene	0.6:1	7.0	0.4	1.1	0.7	1.0	0.4
	0.8:1	5.5	0.6	1.4	0.5	1.2	0.3
	1.2:1	4.3	0.4	1.4	0.4	1.3	0.3
$\alpha$ -Terpineol	0.6:1	15.0	NE <sup>a</sup>	1.4	0.5	1.2	0.3
	0.8:1	16.0	NE	1.3	0.5	1.1	0.3
	1.2:1	5.0	NE	0.7	ND <sup>b</sup>	0.4	ND
Nerolidol	0.6:1	7.7	NE	1.2	0.6	1.0	0.4
	0.8:1	18.0	1.0	1.3	0.5	1.1	0.4
	1.2:1	TE <sup>c</sup>	1.0	TE	TE	TE	TE
Control		18.0	NE	2.7	1.5	1.2	0.4

<sup>a</sup> NE = no extraction.

<sup>b</sup> ND = not determined.

<sup>c</sup> TE = total extraction.

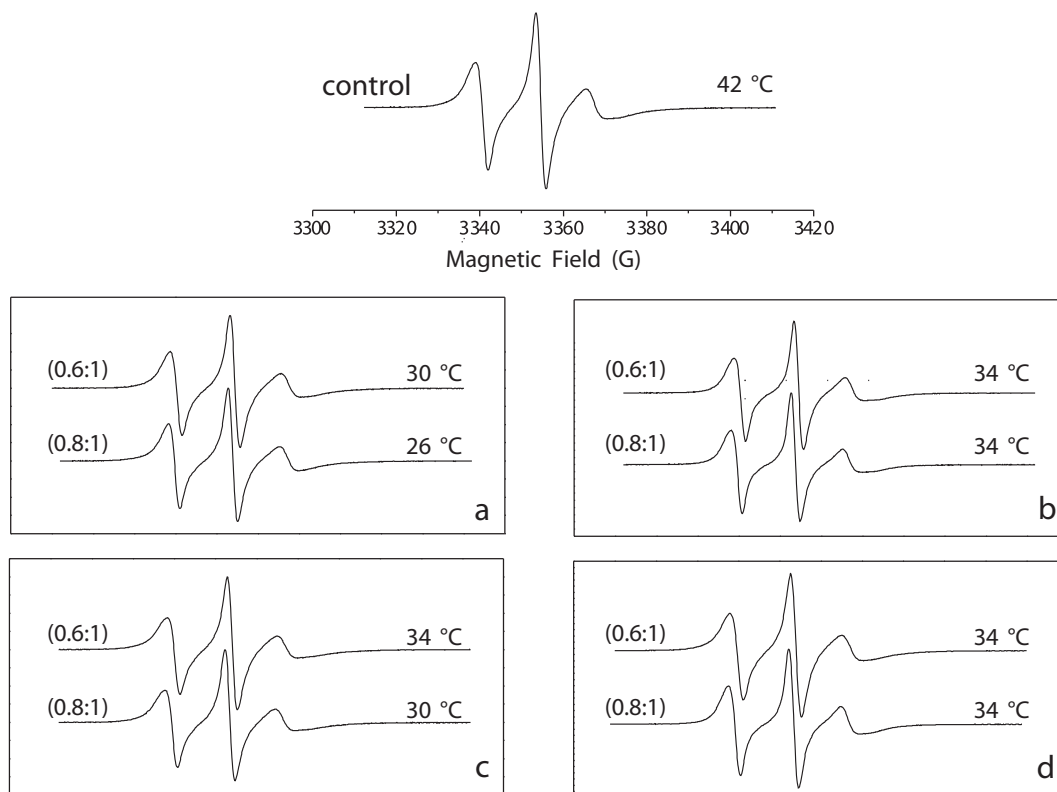


**Fig. 7.** EPR spectra of 5-DMS embedded in DPPC membranes treated with terpenes at a terpene:lipid total molar ratio of 0.8:1. Panels: a, 1,8-cineole; b,  $\alpha$ -terpineol; c, (+)-limonene; d, nerolidol. The spectra shown are those that most closely resemble the spectrum of 5-DMS in pure DPPC at 42 °C (characteristic spectrum of the phase transition).

the highest  $\text{LogP}_{O/W}$ , nerolidol did not extract the membrane lipids at the lower terpene concentration, but nerolidol produced the highest lipid extraction for the 0.8:1 terpene:lipid molar ratio and caused total spin label extraction when applied at the highest evaluated concentration; this finding indicated that the potency for lipid extraction is primarily related to the partitioning of the terpene between membranes

and the aqueous phase. At the lowest evaluated concentration, nerolidol completely penetrated the membrane, as shown by the increase in membrane dynamics (Fig. SM2A) and the population of component 2 (Fig. 8). With its high membrane–water partition coefficient, nerolidol was the terpene that caused the greatest changes in the lipid bilayer, leading to an apparent disintegration at the highest

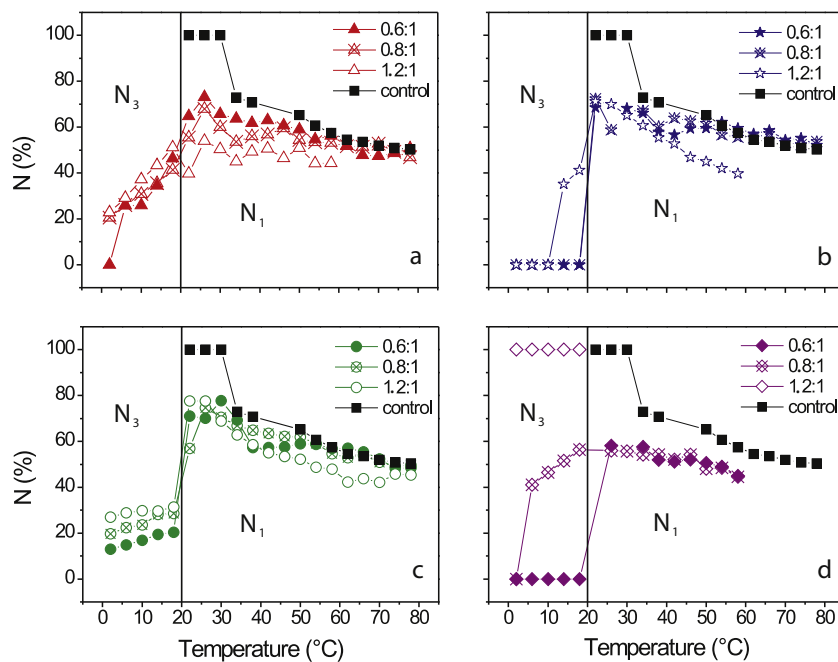


**Fig. 8.** Relative populations of the spin label 5-DMS incorporated into DPPC vesicles treated with terpenes. Panels: a, 1,8-cineole; b,  $\alpha$ -terpineol; c, (+)-limonene; d, nerolidol. The spectra were simulated using components C1 and C3 for temperatures below 20 °C and components C1 and C2 for temperatures above 20 °C.  $N_1$  and  $N_3$  indicate the percentages of spin labels in components 1 and 3, respectively.



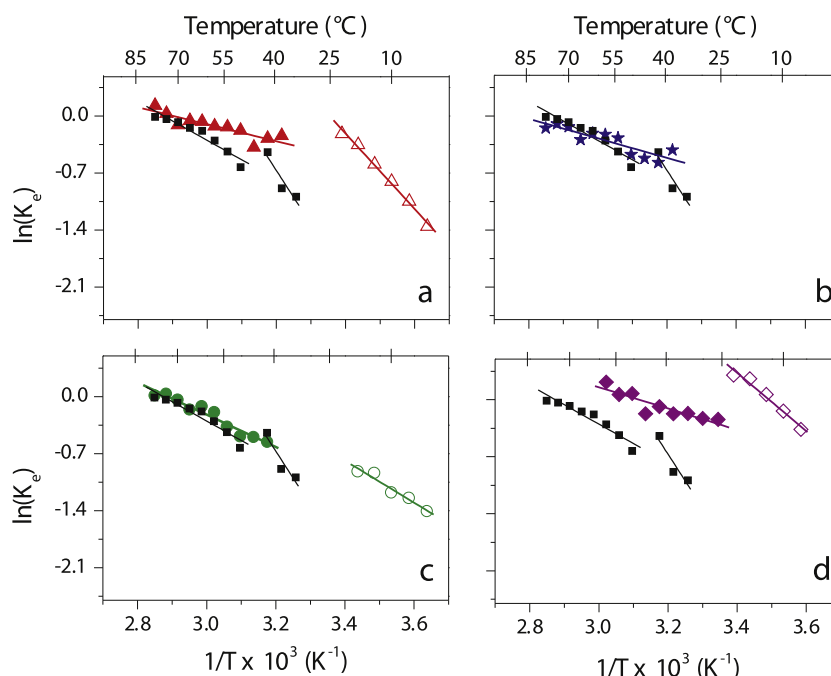


**Fig. 9.** Natural logarithm of the equilibrium constant,  $K_e$ , which was calculated based on the relative populations of 5-DMS incorporated into pure DPPC vesicles (control, black squares) and terpene-treated vesicles at a terpene:lipid total molar ratio of 0.8:1 as a function of the reciprocal of the absolute temperature. Panels: a, 1,8-cineole; b,  $\alpha$ -terpineol; c, (+)-limonene; d, nerolidol. The open and closed symbols represent  $K_e = N_3/N_1$  and  $K_e = N_2/N_1$ , respectively.

concentration. This can be observed in Fig. SM1B-d, in which the spectra of DPPC vesicles treated with the highest nerolidol concentration were all fitted with just one spectral component (component C3). Furthermore, the values of rotational correlation time, depicted in Fig. SM2B-d (open diamonds), were not significantly different from those obtained for the spin label structured into nerolidol micelles (asterisks). This indicates that treatment with nerolidol at 1.2:1 causes DPPC vesicles to lose their lipid bilayer structure. Increasing temperatures led to

greater extraction, as shown in Fig. 8 (from 0 to 20 °C), suggesting that increasing the fluidity of the bilayer facilitates its disruption. An increase in the terpene:lipid molar ratio to 0.8:1 or 1.2:1 also promoted lipid extraction because it results in increased fluidity and lipid spacing in the bilayer. Only limonene and 1,8-cineole were able to extract the spin-labeled lipid at the lowest tested concentration (0.6:1 ratio). Interestingly, these two terpenes are the least polar (polar surface area: limonene = 0 Å<sup>2</sup>; cineole = 9.23 Å<sup>2</sup>;  $\alpha$ -terpineol = 20.23 Å<sup>2</sup>; and nerolidol = 20.23 Å<sup>2</sup>) [31]), and this characteristic may have favored their penetration into the membrane, causing increased fluidity and facilitating the escape of the spin probe.

Recently, EPR spectroscopy showed that the terpenes nerolidol, (+)-limonene,  $\alpha$ -terpineol and 1,8-cineole dramatically increase the molecular dynamics of the lipid component in the plasma membrane of *L. amazonensis* promastigotes at terpene concentrations similar to those that inhibit 50% of the parasite growth [16]. Moreover, at their respective IC<sub>50</sub> values, these terpenes caused the lysis of 4 to 9% of cells, and this percentage reached up to approximately 50% at concentrations two to three times higher than the IC<sub>50</sub> values [16]. The IC<sub>50</sub> values of the sesquiterpene nerolidol and the monoterpenes (+)-limonene,  $\alpha$ -terpineol and 1,8-cineole were 0.008, 0.549, 0.678 and 4.697 mM, respectively [16]. This result demonstrated that the *in vitro* cytotoxicity of nerolidol was similar to that of miltefosine, which is the first effective oral drug approved for the treatment of visceral and cutaneous leishmaniasis [32]. Overall, these IC<sub>50</sub> values and lysis results partially agree with the results obtained in this work. Although nerolidol showed an antiproliferative effect and lysis capacity at very low concentrations and showed the most lipid extraction in this work, 1,8-cineole, which showed an extraction potential similar to that of (+)-limonene in DPPC membranes, showed only a minor effect against *Leishmania*. This finding could be explained if its partition coefficient in the parasite cell membrane is much lower than that in the DPPC bilayer. In a trial comparing the toxicity effects of seven monoterpenes on cultured fibroblasts, 1,8-cineole was the least cytotoxic and also had one of the lowest hemolytic potentials [17]. Interestingly, to simulate the EPR spectra of a spin label in the terpene-treated *Leishmania* plasma membrane, it was necessary to use a model with two spectral

**Table 2**

Change in standard Gibbs free energy ( $\Delta G^\circ$ ), enthalpy ( $\Delta H^\circ$ ) and entropy ( $\Delta S^\circ$ ) associated with the transfer of 5-DMS from component 1 to 3 (temperature range  $\alpha = 0$ –20 °C) and from C1 to C2 (temperature range  $\beta$ – $\gamma = 20$ –80 °C) in pure and terpene-treated DPPC membranes at terpene:lipid total molar ratios of 0.6:1, 0.8:1 and 1.2:1.

Samples		$\Delta G^\circ$		$\Delta H^\circ$		$\Delta S^\circ$	
		(kcal/mol)		(kcal/mol)		(cal/mol K)	
		10 °C					
		C <sub>1</sub> → C <sub>3</sub>	C <sub>1</sub> → C <sub>2</sub>	C <sub>1</sub> → C <sub>3</sub>	C <sub>1</sub> → C <sub>2</sub>	C <sub>1</sub> → C <sub>3</sub>	C <sub>1</sub> → C <sub>2</sub>
0.6:1	1,8-Cineole	0.59	0.34	8.3	3.4	27.6	10.0
	(+)-Limonene	0.90	0.50	6.2	2.0	18.7	5.7
	$\alpha$ -Terpineol	NE <sup>a</sup>	0.41	NE	2.2	NE	6.0
	Nerolidol	NE	0.19	NE	3.2	NE	9.9
0.8:1	1,8-Cineole	0.45	0.08	9.2	2.1	30.9	6.0
	(+)-Limonene	0.66	0.43	5.1	3.9	15.9	11.3
	$\alpha$ -Terpineol	NE	0.43	NE	2.4	NE	6.6
	Nerolidol	0.08	0.10	7.1	2.6	24.8	8.1
1.2:1	1,8-Cineole	0.29	0.12	13.0	1.6	44.7	5.2
	(+)-Limonene	0.48	0.23	2.7	3.2	7.7	9.9
	$\alpha$ -Terpineol	ND <sup>b</sup>	ND	ND	ND	SE	ND
	Nerolidol	TE <sup>c</sup>	TE	TE	TE	TE	TE
Control (26–41 °C)		–	0.60	–	13.1	–	40.6
Control (46–78 °C)		–	0.30 <sup>d</sup>	–	4.7	–	13.6

The values were calculated based on Eq. (4), using the data in Fig. 9.

<sup>a</sup> NE = not cause extraction.

<sup>b</sup> ND = not determined (experimental data insufficient to calculate the thermodynamic parameters safely).

<sup>c</sup> TE = total extraction.

<sup>d</sup>  $\Delta G^\circ$  was calculated at 50 °C.

components. Collectively, these results demonstrated that terpenes also cause the formation of two components in a cell membrane and that an increase in the terpene concentration leads to an increase in the population of the most dynamic spin probe component [16].

## 5. Conclusions

EPR spectroscopy has contributed significantly to the understanding of the cellular membrane. In this work, EPR spectroscopy provided additional information on the behavior of a spin-labeled lipid inserted into a DPPC lipid bilayer, which must also be studied using other techniques. In particular, we show the formation of two spectral components in which a spin-labeled lipid can incorporate into the bilayer in structural environments of very different mobilities. We also demonstrate that the terpene molecules act as lipid spacers, leading to an increase in the population of the more mobile component. Thus, the insertion of terpenes into the lipid bilayer increased the fluidity and substantially reduced the temperature of the main phase transition of DPPC membranes. It has been shown that terpenes can also act as extractors of a spin-labeled lipid; this extraction is enhanced for terpenes with high membrane–water partition coefficients and for terpenes that can form highly hydrophobic micellar structures that are sufficiently dynamic to compete for membrane lipids. Of the four studied terpenes,  $\alpha$ -terpineol, which has the lowest octanol–water partition coefficient and formed the most rigid micelles, was the terpene that extracted the smallest fraction of spin label. In contrast, (+)-limonene formed more fluid micelles and, with its high membrane–water partition coefficient, extracted the spin probe from the membrane at all three evaluated concentrations. With the highest membrane–water partition coefficient, nerolidol caused high extraction at the intermediate concentration and disrupted the membrane when applied at the highest concentration. In addition to being potent skin permeation enhancers, terpenes have antiparasitic and antineoplastic activities that are most likely due to their effects on the lipid component of the cell membrane.

Fig. SM1 shows the most representative experimental EPR spectra, their best-fit spectra and the corresponding spectral components of 5-DMS incorporated into terpene-treated DPPC membranes at three different temperatures and two terpene concentrations. For the temperature range  $\alpha$ , the spectra of the membranes treated with 1,8-cineole, (+)-limonene and nerolidol can be described as the superposition of components C1/C3 and C1/C2 at the terpene:lipid total molar ratio of 0.6:1, whereas at the molar ratio of 1.2:1, the spectra can be fitted by a combination of C1/C3 for 1,8-cineole and (+)-limonene and by C3 alone for nerolidol. For  $\alpha$ -terpineol, the EPR spectra can be fitted using C1 for the molar ratio of 0.6:1 and C1/C3 for the ratio of 1.2:1. For the temperature range  $\beta$ , all of the spectra of the DPPC membranes can be fitted using the combination of C1 and C2, except for the spectra of  $\alpha$ -terpineol (C1/C3) and nerolidol (C3) for the 1.2:1 molar ratio. For the temperature range  $\gamma$  and the molar ratio of 0.6:1, the spectra for all terpenes can be fitted using a combination of C1 and C2. For the 1.2:1 molar ratio, the spectra of 1,8-cineole and (+)-limonene were fitted using C1/C2, the  $\alpha$ -terpineol spectra were fitted using C1/C3, and the nerolidol spectra were fitted with C3 alone. Fig. SM2 shows the thermal behavior of the rotational correlation time as a function of temperature for DPPC vesicles treated with terpenes at the molar ratios of 0.6:1 and 1.2:1.

## Acknowledgments

This work was financially supported by grants from the Brazilian research funding agencies CNPq (564276/2010-3), CAPES and FAPESP (564276/2010-3). Sebastião Antonio Mendanha was the recipient of a fellowship from the CAPES. Antonio Alonso is the recipient of a research grant from CNPq.

## References

- [1] D.J. Mcgarvey, R. Croteau, Terpenoid metabolism, *Plant Cell* 7 (1995) 1015–1026.
- [2] P.L. Crowell, Prevention and therapy of cancer by dietary monoterpenes, *J. Nutr.* 129 (1999) 775S–778S.
- [3] M.N. Gould, Cancer chemoprevention and therapy by monoterpenes, *Environ. Health Perspect.* 105 (Suppl. 4) (1997) 977–979.
- [4] S. Bardon, V. Foussard, S. Fournel, A. Loubat, Monoterpenes inhibit proliferation of human colon cancer cells by modulating cell cycle-related protein expression, *Cancer Lett.* 181 (2002) 187–194.
- [5] T. Rabi, A. Bishayee, Terpenoids and breast cancer chemoprevention, *Breast Cancer Res. Treat.* 115 (2009) 223–239.
- [6] H. Yang, Q.P. Dou, Targeting apoptosis pathway with natural terpenoids: implications for treatment of breast and prostate cancer, *Curr. Drug Targets* 11 (2010) 733–744.
- [7] R.J. Thoppil, A. Bishayee, Terpenoids as potential chemopreventive and therapeutic agents in liver cancer, *World J. Hepatol.* 27 (2011) 228–249.
- [8] C.S. Wu, Y.J. Chen, J.J. Chen, J.J. Shieh, C.H. Huang, P.S. Lin, G.C. Chang, J.T. Chang, C.C. Lin, Terpinen-4-ol induces apoptosis in human nonsmall cell lung cancer in vitro and in vivo, *Evid. Based Complement. Alternat. Med.* 2012 (2012) 818261.
- [9] B. Oliva, E. Piccirilli, T. Ceddia, E. Pontieri, P. Aureli, A.M. Ferrini, Antimycotic activity of *Melaleuca alternifolia* essential oil and its major components, *Lett. Appl. Microbiol.* 37 (2003) 185–187.
- [10] D.C. Arruda, D.C. Miguel, J.K. Yokoyama-Yasunaka, A.M. Katzin, S.R. Uliana, Inhibitory activity of limonene against *Leishmania* parasites in vitro and in vivo, *Biomed. Pharmacother.* 63 (2009) 643–649.
- [11] D.C. Arruda, F.L. D'Alexandri, A.M. Katzin, S.R. Uliana, Antileishmanial activity of the terpene nerolidol, *Antimicrob. Agents Chemother.* 49 (2005) 1679–1687.
- [12] J.L.V. dos Anjos, D. de Sousa Neto, A. Alonso, Effects of ethanol/l-menthol on the dynamics and partitioning of spin-labeled lipids in the stratum corneum, *Eur. J. Pharm. Biopharm.* 67 (2007) 406–412.
- [13] J.L.V. dos Anjos, D.S. Neto, A. Alonso, Effects of 1,8-cineole on the dynamics of lipids and proteins of stratum corneum, *Int. J. Pharm.* 345 (2007) 81–87.
- [14] J.L.V. dos Anjos, A. Alonso, Terpenes increase the partitioning and molecular dynamics of an amphipathic spin label in stratum corneum membranes, *Int. J. Pharm.* 350 (2008) 103–112.
- [15] H.S. Camargos, A.H. Silva, J.L.V. Anjos, A. Alonso, Molecular dynamics and partitioning of di-tert-butyl nitroxide in stratum corneum membranes: effect of terpenes, *Lipids* 45 (2010) 419–427.
- [16] H.S. Camargos, R.A. Moreira, S.A. Mendanha, K.S. Fernandes, M.L. Dorta, A. Alonso, Terpenes increase the lipid dynamics in the *Leishmania* plasma membrane at concentrations similar to their  $IC_{50}$  values, *PLoS ONE* 9 (2014) e104429.
- [17] S.A. Mendanha, S.S. Moura, J.L.V. Anjos, M.C. Valadares, A. Alonso, Toxicity of terpenes on fibroblast cells compared to their hemolytic potential and increase in erythrocyte membrane fluidity, *Toxicol. in Vitro* 27 (2013) 323–329.
- [18] D.E. Budil, S. Lee, S. Saxena, J.H. Freed, Nonlinear-least-squares analysis of slow-motion EPR spectra in one and two dimensions using a modified Levenberg–Marquardt algorithm, *J. Magn. Reson. Ser. A* 120 (1996) 155–189.
- [19] D.J. Schneider, J.H. Freed, *Biological Magnetic Resonance*, vol. 8, Plenum, New York, 1989, 1–76.
- [20] A. Alonso, J. Vasques da Silva, M. Tabak, Hydration effects on the protein dynamics in stratum corneum as evaluated by EPR spectroscopy, *Biochim. Biophys. Acta* 1646 (2003) 32–41.
- [21] W.P. de Queirós, D. de Sousa Neto, A. Alonso, Dynamics and partitioning of spin-labeled stearamides into the lipid domain of stratum corneum, *J. Control. Release* 106 (2005) 374–385.
- [22] H.S. Camargos, A. Alonso, Electron paramagnetic resonance (EPR) spectral components of spin-labeled lipids in saturated phospholipid bilayers: effect of cholesterol, *Quim Nova* 36 (2013) 815–821.
- [23] T. Róg, L.M. Stimson, M. Pasenkiewicz-Gierula, I. Vattulainen, M. Karttunen, Replacing the cholesterol hydroxyl group with the ketone group facilitates sterol flip-flop and promotes membrane fluidity, *Phys. Chem. B* 112 (7) (2008) 1946–1952. <http://dx.doi.org/10.1021/jp075078h>.
- [24] S. Mabrey, J.M. Sturtevant, Investigation of phase transitions of lipids and lipid mixtures by sensitivity differential scanning calorimetry, *Proc. Natl. Acad. Sci. U. S. A.* 73 (1976) 3862–3866.
- [25] W. Greiner, L. Neise, H. Stöcker, *Thermodynamics and Statistical Mechanics*, Springer-Verlag, 1995.
- [26] P. Atkins, J. de Paula, *Physical Chemistry*, W. H. Freeman, 2006.
- [27] H.K. Vaddi, P.C. Ho, Y.W. Chan, S.Y. Chan, Terpenes in ethanol: haloperidol permeation and partition through human skin and stratum corneum changes, *J. Control. Release* 81 (1–2) (2002 May 17) 121–133.
- [28] K.S. Bhatia, J. Singh, Mechanism of transport enhancement of LHRH through porcine epidermis by terpenes and iontophoresis: permeability and lipid extraction studies, *Pharm. Res.* 15 (12) (1998 Dec) 1857–1862.
- [29] P. Karande, A. Jain, K. Ergun, V. Kispersky, S. Mitragotri, Design principles of chemical penetration enhancers for transdermal drug delivery, *Proc. Natl. Acad. Sci. U. S. A.* 102 (2005) 4688–4693.
- [30] A.K. Jain, N.S. Thomas, R. Panchagnula, Transdermal drug delivery of imipramine hydrochloride: I. Effect of terpenes, *J. Control. Release* 79 (2002) 93–101.
- [31] ChemAxon, <http://www.chemicalize.org/10> 2014.
- [32] R.A. Moreira, S.A. Mendanha, K.S. Fernandes, G.G. Matos, L. Alonso, M.L. Dorta, A. Alonso, Miltefosine Increases Lipid and Protein Dynamics in *Leishmania amazonensis* Membranes at Concentrations Similar to Those Needed for Cytotoxicity Activity Antimicrobial agents and chemotherapy 58 (6), 3021–3028.